Cationic copolymer enhances 8-17 DNAzyme and MNAzyme activities

Journal:	*Biomaterials Science*
Manuscript ID	BM-ART-03-2020-000428.R1
Article Type:	Paper
Date Submitted by the Author:	29-Apr-2020
Complete List of Authors:	Rudeejaroonrung, Krittika; Tokyo Institute of Technology, Life Science and Technology Hanpanich, Orakan; Tokyo Institute of Technology, Life Science and Technology Saito, Ken; Tokyo Institute of Technology, Life Science and Technology Shimada, Naohiko; Tokyo Institute of Technology, Maruyama, Atsushi; Tokyo Institute of Technology, Life Science and Technology

SCHOLARONE™
Manuscripts

Cationic copolymer enhances

8-17 DNAzyme and MNAzyme activities

Krittika Rudeejaroonrung, Orakan Hanpanich, Ken Saito, Naohiko Shimada,

Atsushi Maruyama*

School of Life Science and Technology, Tokyo Institute of Technology, 4259-

B57 Nagatsuta-cho, Midori, Yokohama, Kanagawa 226-8501, Japan

*Corresponding Author   *E-mail:* amaruyama@bio.titech.ac.jp

Abstract

DNAzymes are DNA molecules capable of catalytic activity. The catalytic

core of DNAzymes can be separated and conjugated with target binding arms to

create allosteric DNAzymes known as multi-component nucleic acid enzymes

(MNAzymes). Two widely used DNAzymes are the 10-23 and the 8-17

DNAzymes. These DNAzymes differ in catalytic core structures, cleavage sites,

and reactive metal ion cofactors. Previously we showed that the presence of a

cationic comb-type polymer poly(L-lysine)-*graft*-dextran (PLL-*g*-Dex) improved

activities of the 10-23 DNAzyme and MNAzyme by facilitating assembly of the

catalytic complex. In this work, we demonstrate that PLL-*g*-Dex enhances

activities of the 8-17 DNAzyme and MNAzyme; poly(allylamine)-*graft*-dextran and cationic homopolymers did not enhance activities. Metal ion and pH dependences were observed in the presence of PLL-*g*-Dex, suggesting that the cationic copolymer did not impede the interaction between metal ion and the DNA-based enzymes. Thus, PLL-*g*-Dex has chaperone-like activity for DNAzymes and MNAzymes regardless of structures, cleavage sites, and cofactors.

Introduction

The spread of infectious diseases such as severe acute respiratory syndrome (SARS), Middle East respiratory syndrome (MERS), and, most recently, the coronavirus-caused disease COVID-19, has focused attention on outbreak control. Critical to epidemic control is timely diagnosis; therefore, simple, fast, and accurate methods to detect pathogens are required. In addition to conventional PCR-based methods, simpler isothermal amplification methods such as rolling circle amplification and loop-mediated isothermal amplification can also be used for the detection of pathogen genetic materials or disease

markers.[1–3] These strategies often have complicated designs and require specialized

equipment.

Deoxyribozymes (DNAzymes), originally introduced by Breaker and Joyce

in 1994, are DNA molecules capable of catalyzing a reaction such as

phosphodiester bond cleavage.[4] DNAzymes offer several advantages over

ribozymes and protein enzymes including high stability and straightforward

preparation.[5] The RNA-cleaving DNAzymes consist of a catalytic core and

substrate binding arms that can be customized to bind and cleave an RNA

substrate of a desired sequence.[6] One of the ongoing DNAzymes applications is

metal sensing.[7] DNAzyme applications were broadened by development of

multicomponent nucleic acid enzymes (MNAzymes). MNAzymes are allosteric

DNAzymes with activities that can be regulated via target binding.[8] MNAzymes

are engineered by splitting the catalytic core of a DNAzyme into two parts and

conjugating each part with a target binding arm.[9] In the presence of target nucleic

acid, the MNAzyme complex assembles to form a catalytically active structure

that can cleave multiple substrates. MNAzymes have been used to amplify signal

isothermally. Because MNAzymes are simple to design and highly specific for

particular substrate and target sequences, they have been integrated as detection units in DNA-based nanotechnologies including biosensors.[10–13]

Our group has extensively studied the cationic comb-type copolymer poly(L-lysine)-*graft*-dextran (PLL-*g*-Dex) (Fig. 1A), which is composed of a cationic backbone and hydrophilic graft chains (reviewed in [14]). The copolymer exhibits nucleic acid chaperone-like activity as it is capable of promoting hybridization of complementary strands[15–18] and facilitating strand exchange reactions.[19–22] We recently reported that the copolymer remarkably enhances the reaction rate of 10-23 DNAzymes[23,24] (Fig. 1B) and 10-23 MNAzymes[25,26] (Fig. 1C) when Mn^{2+} is the metal ion cofactor. The copolymer stabilizes 10-23 DNAzyme and 10-23 MNAzyme complexes without slowing dissociation; consequently, the copolymer improves turnover rate under multiple-turnover conditions. This is a unique feature of PLL-*g*-Dex, as in the presence of another cationic comb-type polymer, poly(allylamine)-graft-dextran (PAA-*g*-Dex) (Fig. 1D), the activity of the 10-23 DNAzyme is reduced.[24]

Like the 10-23 DNAzymes, 8-17 DNAzymes are also widely used RNA-cleaving DNAzymes (Fig. 1E).[5] MNAzymes have also been designed based on the 8-17 DNAzyme catalytic core (Fig. 1F). The 10-23 MNAzymes are more

catalytically active than are the 8-17 MNAzymes, whereas the corresponding DNAzymes cleave substrates with similar efficiencies.[9,27] The 10-23 DNAzyme catalytic core is composed of an unstructured loop, whereas that of the 8-17 DNAzyme is composed of a three base-pair stem, an AGC trinucleotide loop, and a WCGR(A) loop (where W=A/T, and R=A/G).[28] Tertiary structure formation is crucial for catalytic efficiency of DNAzymes. We reasoned that PLL-*g*-Dex should facilitate the association and stabilization of the more complicated structures of 8-17 MNAzymes, as it does that of the 10-23 MNAzyme, and improve the reaction rates.

In 1997, Santaro and Joyce showed that the 10-23 DNAzymes cleave almost any purine-pyrimidine bond (5'-RY-3', where R=rA/rG, and Y=rU/rC) in an all-RNA substrate but that the 8-17 DNAzymes are able to cleave only the riboadenine-riboguanine linkage (5'-rArG-3').[5] Later studies showed that the 8-17 DNAzyme is able to cleave a single ribonucleotide-containing DNA substrate and cleaves between more than half of all 16 dinucleotides, although the efficiency varied considerably.[29,30] The ability of the 8-17 DNAzyme to cleave many dinucleotide junctions indicate that this DNAzyme and its corresponding

MNAzyme should be more broadly applicable than the 10-23 DNAzyme and MNAzyme.

In order to improve the cleavage activities of DNAzymes and MNAzymes, the copolymer must not disrupt the interaction of a divalent cation with the catalytic core and must not collapse the catalytically active structure.[23] Here, we demonstrate that PLL-*g*-Dex enhances the activity of 8-17 DNAzymes and 8-17 MNAzymes and enables recognition of DNA and RNA targets. Thus, despite the differences between the 8-17 and the 10-23 enzymes in catalytic core structures, cleavage sites, and metal ion cofactors, PLL-*g*-Dex facilitates complex assembly and promotes turnover increasing the rates of the catalyzed reactions.
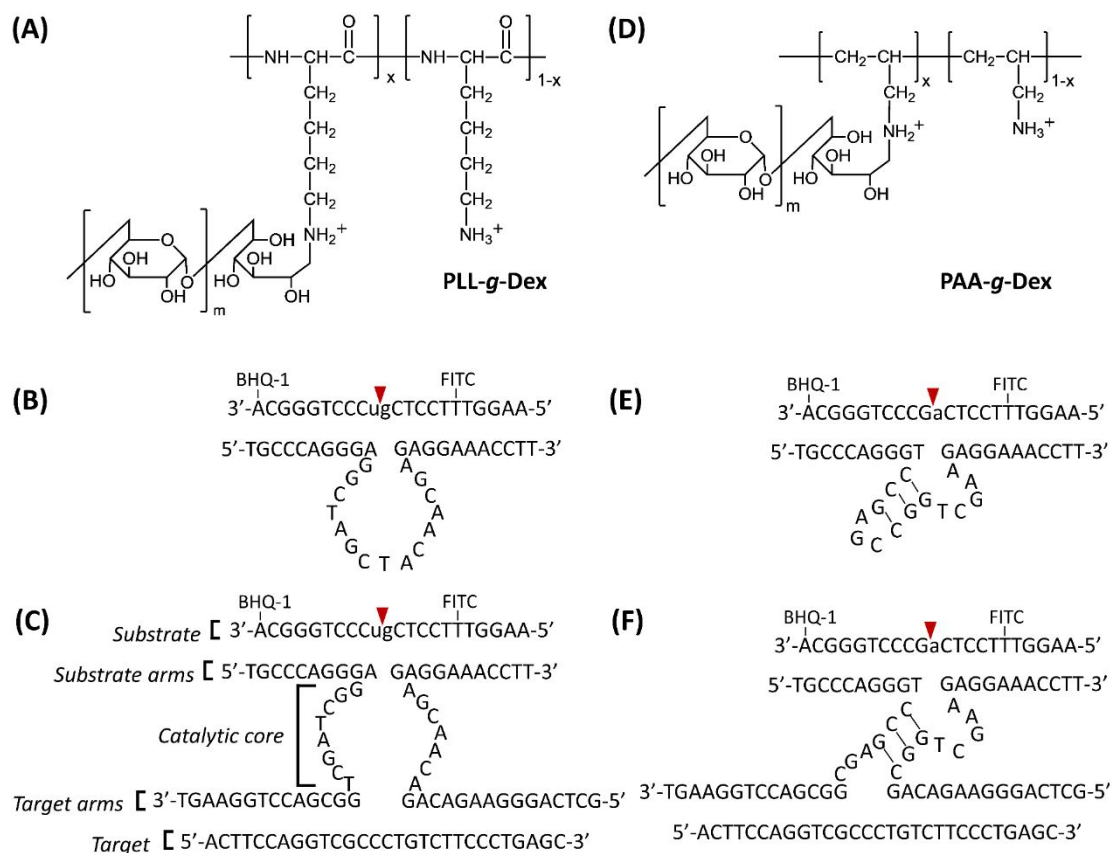
Figure 1. (A) Structural formula of PLL-*g*-Dex. (B, C) Sequences and locations of fluorophore and quencher on B) 10-23 DNAzyme and C) 10-23 MNAzyme used in previous studies. Lowercase letters denote ribonucleotides and the red triangles indicate the cleavage sites on the substrates. (D) Structural formula of PAA-*g*-Dex. (E, F) Sequences and locations of fluorophore and quencher on E) 8-17 DNAzyme and F) 8-17 MNAzyme used in this study. Lowercase letters denote ribonucleotides and the red triangles indicate the cleavage sites on the substrates.

Experimental

Materials

All HPLC-grade oligonucleotides in this study were obtained from Fasmac and were used without further purification. Sodium hydroxide, sodium chloride, magnesium sulfate, and lead (II) acetate were purchased from Wako Pure Chemical Industries. 2-[4-(2-Hydroxyethyl)piperazin-1-yl]ethanesulfonic acid (HEPES) was obtained from Nacalai Tesque. Poly($_L$-lysine) hydrobromide (PLL·HBr, M_w= 7.5 x 10^3) was purchased from Sigma-Aldrich and poly(allylamine) hydrochloride (PAA·HCl, M_w= 5 x 10^3) was purchased from Nittobo. Dextran (Dex, M_w= 8.0 x 10^3 – 1.2 x 10^4) was obtained from Funakoshi. The cationic comb-type copolymers, PLL-*g*-Dex and PAA-*g*-Dex were prepared according to previously published procedures.[17] In brief, the copolymers were synthesized by a reductive amination reaction of dextran with either PLL or PAA. The copolymers were purified by ion-exchange chromatography column followed by dialysis and lyophilization. Copolymers were characterized using ^{1}H NMR and GPC.

Methods

The cleavage of the substrate was monitored by observing Förster

resonance energy transfer (FRET) under multiple-turnover conditions. Unless

stated otherwise, substrate (final concentration: 100 nM), DNAzyme or

MNAzyme parts (final concentration: 20 nM), and target (for MNAzyme only,

final concentration: 20 nM) were dissolved in a buffer containing 50 mM HEPES

and 150 mM NaCl at pH 7.3. The solution was pre-incubated at the desired

reaction temperature in a cuvette. After 5 minutes, the copolymer (ratio of

positively charged amino group of copolymer to negatively charged phosphate

group of nucleic acids (N/P ratio) of 2) was injected into the solution. N/P ratio of

2 allows complete complex formation between the copolymer and nucleic acids

(Fig. S1).[24] The metal ion cofactors (Pb^{2+} final concentration 0.2 mM; Mg^{2+} final

concentration 25 mM) were injected at 1 minute after polymer injection to start

the reaction. The fluorescence intensity was measured using an FP-6500

spectrofluorometer (Jasco) at an excitation wavelength (λ_{ex}) 494 nm and an

emission wavelength (λ_{em}) 520 nm. The substrate cleavage percentage (%

cleavage) over time was calculated using the following equation: *% cleavage =

$(I_t - I_0)/(I_\infty - I_0)$, where I_t is the fluorescence intensity at reaction time t, I_∞ is the*

fluorescence intensity at complete reaction, and I_0 is the initial fluorescence intensity before metal ion injection. The observed rate constant (k_{obs}) was calculated by fitting the experimental data to the following equation: $I_t = I_0 + (I_\infty - I_0)(1 - e^{-k_{obs}})$.
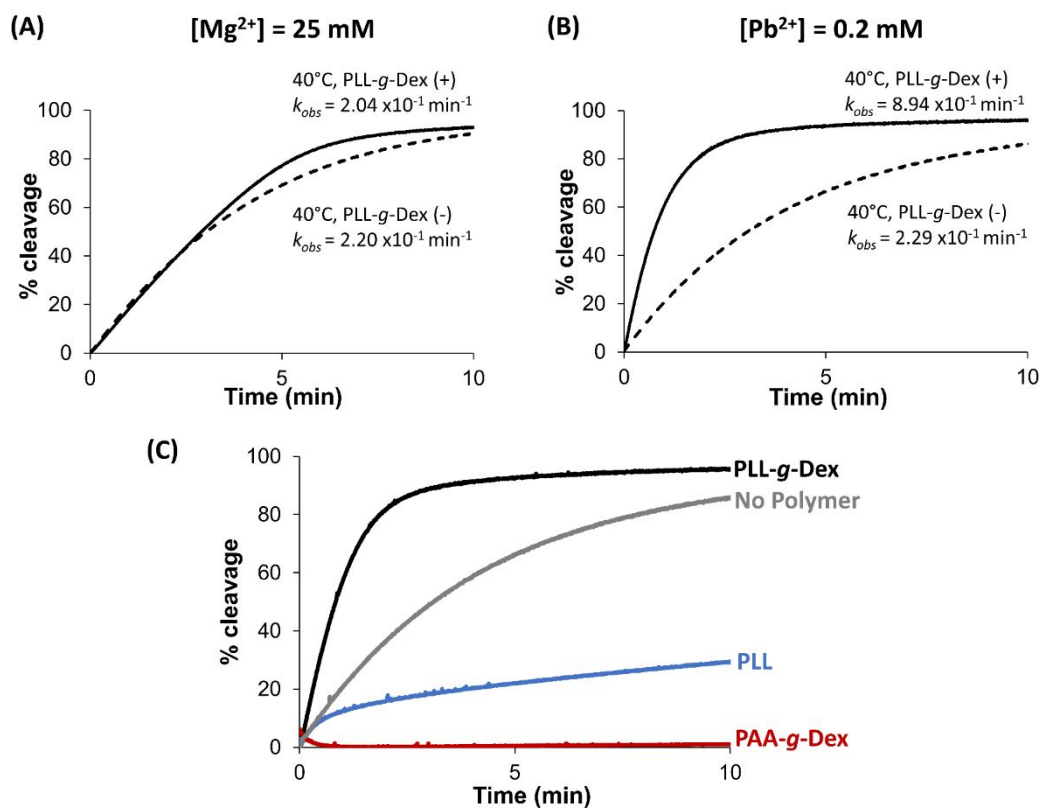
Results and discussion

Copolymer and metal ion cofactor influence DNAzyme rate-determining step

In order to examine the effect of cationic copolymer on the catalytic core functions, we initially used the 8-17 DNAzyme variant usually known as 17E (Fig. 1E).[27,28] The 8-17 DNAzymes were developed through an *in vitro* selection procedure and their cleavage activities are Mg^{2+} ion dependent.[5] In order to examine the influence of the copolymer under the similar ionic concentration to our prior works, we firstly investigated the effect of PLL-*g*-Dex in the presence of 25 mM Mg^{2+} (as previously used in our earlier study[25]) under multiple-turnover conditions. At the optimal temperature, 40 °C, the observed rate constants (k_{obs}) without and with the copolymer were 2.20×10^{-1} min^{-1} and 2.04×10^{-1} min^{-1}, respectively (Fig. 2A). The fact that these rate constants did not differ considerably indicated that when Mg^{2+} was metal ion cofactor, the rate-limiting step was the cleavage reaction rather than turnover. Under these conditions, the cationic copolymer may facilitate DNAzyme·substrate complex assembly, but the overall reaction rate is limited by the rate of the cleavage reaction.

Although 8-17 DNAzymes were originally reported to be Mg^{2+} dependent, Pb^{2+} is a better metal ion cofactor for 8-17 DNAzymes.[31] Since the maximum Pb^{2+}

concentration used with 8-17 DNAzymes was 0.2 mM [27], we monitored the reaction in the presence of 0.2 mM Pb^{2+} in the presence and absence copolymer under multiple-turnover conditions (Fig. 2B). Without the copolymer, k_{obs} in the presence of Pb^{2+} was 2.29 x 10^{-1} min^{-1}, which was not significantly different from that in the presence of Mg^{2+}. However, in the presence of copolymer, the DNAzyme activity almost quadrupled to 8.94 x 10^{-1} min^{-1} at the optimal temperature. With Pb^{2+} as the metal ion cofactor in the absence of copolymer, the rate-limiting step was formation of DNAzyme·substrate complex. The addition of cationic copolymer promoted DNAzyme·substrate complex assembly, which consequently enhanced the reaction rate under the multiple-turnover conditions.

(A) [Mg²⁺] = 25 mM

40°C, PLL-*g*-Dex (+)
k_{obs} = 2.04 x10⁻¹ min⁻¹

40°C, PLL-*g*-Dex (-)
k_{obs} = 2.20 x10⁻¹ min⁻¹

(B) [Pb²⁺] = 0.2 mM

40°C, PLL-*g*-Dex (+)
k_{obs} = 8.94 x10⁻¹ min⁻¹

40°C, PLL-*g*-Dex (-)
k_{obs} = 2.29 x10⁻¹ min⁻¹

(C)

PLL-*g*-Dex
No Polymer
PLL
PAA-*g*-Dex

Figure 2. (A, B) Percent cleavage over time by the 8-17 DNAzyme at pH 7.3 under multiple-turnover conditions at 40 °C in the absence (dotted line) and presence (N/P=2) (solid line) of PLL-*g*-Dex with A) 25 mM Mg²⁺ and B) 0.2 mM Pb²⁺. (C) Percent cleavage over time by the 8-17 DNAzyme under the multiple turnover conditions at pH 7.3 at 40 °C in the absence of polymer (grey line) and in the presence of PLL-*g*-Dex (black line), PLL (blue line), and PAA-*g*-Dex (red line) at N/P =2.

PLL-*g*-Dex enhances 8-17 DNAzyme activity, whereas PAA-*g*-Dex inhibits it

We next compared the effects of PLL-*g*-Dex, the homopolymer PLL, and the cationic comb-type copolymer PAA-*g*-Dex (Fig. 1D), which has a polyallylamine backbone, on the 8-17 DNAzyme activity under multiple-turnover conditions in the presence of 0.2 mM Pb^{2+}. Compared to the reaction without polymers, the addition of PLL-*g*-Dex increased the reaction rate, whereas the addition of PLL homopolymer decreased the reaction rate (Fig. 2C). The lower reaction rate in the presence of PLL was due to the aggregation of the DNA strands caused by interaction with this cationic homopolymer.[32] Interestingly, PAA-*g*-Dex inhibited the reaction to a greater extent than PLL, although the former caused no aggregation of DNA.

A previous study showed that the cleavage rates of DNAzymes depend on the helical conformation adopted by the DNAzyme·substrate complex. Higher substrate cleavage rates were observed when the duplex formed by the DNAzyme with the substrate was a B-form-like helix rather than an A-form-like helix.[33] In one of our early studies of cationic polymers, we found that PAA-*g*-Dex induces B-to-A transitions of DNA duplexes by dehydrating the DNA strands, whereas the DNA duplex remains in a B-form conformation in the presence of

PLL-*g*-Dex.[32,34] We speculate that the DNA duplex in the DNAzyme·substrate complex undergoes a B-to-A transition in the presence of PAA-*g*-Dex, which diminishes the DNAzyme catalytic efficiency (Fig. 2C). We previously reported that PAA-*g*-Dex reduces the activity of the 10-23 DNAzyme.[24] The inhibitory effect of PAA-*g*-Dex on the 8-17 DNAzyme was significantly stronger than that on 10-23 DNAzyme. These results suggested that the 8-17 DNAzyme is more susceptible to conformational changes induced by interactions with cationic copolymers than is the 10-23 DNAzyme.

PLL-*g*-Dex enhances allosteric 8-17 MNAzyme activity

We next investigated the effect of PLL-*g*-Dex on the allosteric 8-17 MNAzyme (Fig. 1F). The target in this study was a DNA strand of 29 nucleotides. The temperature dependence of MNAzyme reaction under the multiple-turnover conditions in the absence and presence of cationic copolymer was evaluated. In the absence of copolymer, reaction rates in the presence of 25 mM Mg^{2+} were higher than those in the presence of 0.2 mM Pb^{2+} (Fig. 3A). This was not the case in the 8-17 DNAzyme reaction. Because proper complex assembly is crucial for catalytic activity of the MNAzyme, we speculate that reaction rates are higher in 25 mM Mg^{2+}, conditions in which MNAzyme assembly is more effective than 0.2

mM Pb^{2+}.[35] To further elucidate this assumption, we investigated the MNAzyme reaction at lower Mg^{2+} concentration. As expected, in the absence of the copolymer, the reaction rates in 10 mM Mg^{2+} were lower than in 25 mM Mg^{2+}, but still higher than in 0.2 mM Pb^{2+} (Fig. S2A). We were unable to increase Pb^{2+} concentration, because precipitation of the nucleic acid occurs at Pb^{2+} concentrations higher than 0.2 mM.[36]

At the optimal temperature in 25 mM Mg^{2+} in the presence of PLL-*g*-Dex, the reaction rate was higher by approximately 3-fold than in the absence of copolymer (Fig. 3B). Likewise, at the optimal temperature in 10 mM Mg^{2+} in the presence of PLL-*g*-Dex, the reaction rate was higher by approximately 2.5-fold than in the absence of copolymer (Fig. S2B). The change in Mg^{2+} concentration did not drastically affect the enhancement ratio by the copolymer, since Mg^{2+} was not the most reactive metal ion cofactor, and was less effective than PLL-*g*-Dex as the assembly facilitator. When Pb^{2+} was the metal ion cofactor, the reaction rate at the optimal temperature was higher by approximately 100-fold in the presence of copolymer; the k_{obs} was 0.24 x 10^{-2} min^{-1} in the absence and 2.39 x 10^{-1} min^{-1} in the presence of copolymer (Fig. 3C). PLL-*g*-Dex had considerably more effect on activity of the MNAzyme than on that of the DNAzyme, especially when Pb^{2+} was

the cofactor. The cationic copolymer facilitated more profoundly the four-stranded

MNAzyme assembly than the two-stranded DNAzyme assembly.
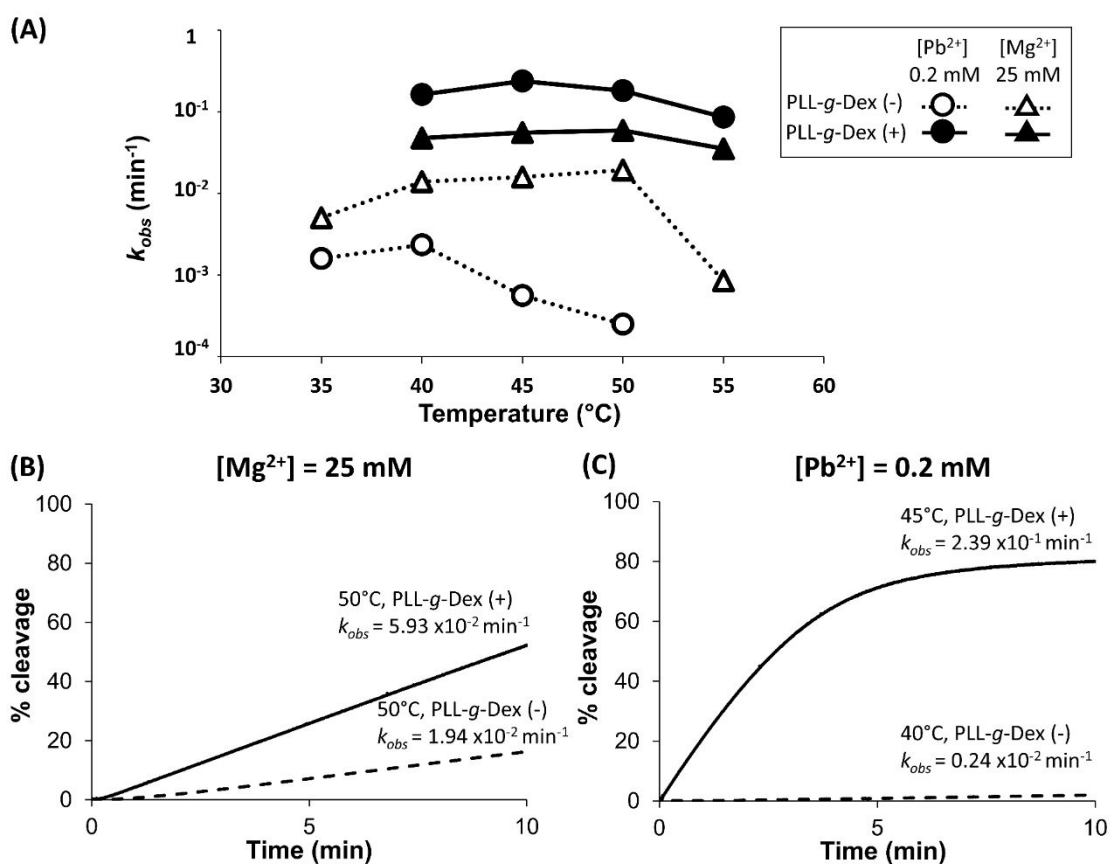
Figure 3. (A) Temperature dependence of k_{obs}, estimated in 25 mM Mg^{2+} (triangles) and in 0.2 mM Pb^{2+} (circles) in the absence (dotted line) and presence (solid line) of PLL-*g*-Dex. (B, C) Percent cleavage of substrate by 8-17 MNAzyme with 29-nt-long DNA target reactions at pH 7.3 under multiple-turnover conditions at the optimal temperature in the absence (dotted line) and presence (N/P=2) (solid line) of PLL-*g*-Dex with B) 25 mM Mg^{2+} and C) 0.2 mM Pb^{2+}.

To determine whether the detection of target nucleic acid by the 8-17 MNAzyme is enhanced by the presence of PLL-g-Dex, we evaluated detection of microRNA-21 (miR-21), a biomarker of several diseases including cancer.[37–39] In the detection system used, a fluorophore and a quencher in the substrate are separated upon cleavage of the substrate, which only occurs upon proper assembly of the MNAzyme on the target miR-21 (Fig. 4A). Under multiple-turnover conditions with 0.2 mM Pb^{2+} as a metal ion cofactor, the reaction rate was 0.09×10^{-2} min^{-1} at the optimal temperature of 20 °C. In the presence of copolymer, the rate was 6.54×10^{-2} min^{-1} at the optimal temperature of 35 °C (Fig. 4B); this is more than 70 times higher than the rate in the absence of copolymer. The optimal temperature increased from 20 °C to 35 °C when the cationic copolymer was introduced (Fig. 4B). We previously reported that PLL-g-Dex increased the thermal stability of 10-23 MNAzyme.[26] The experiment described here suggests that the copolymer also stabilized the 8-17 MNAzyme complex, which in turn increased optimal reaction temperature and the reaction rate.[26]

(A)

(B)
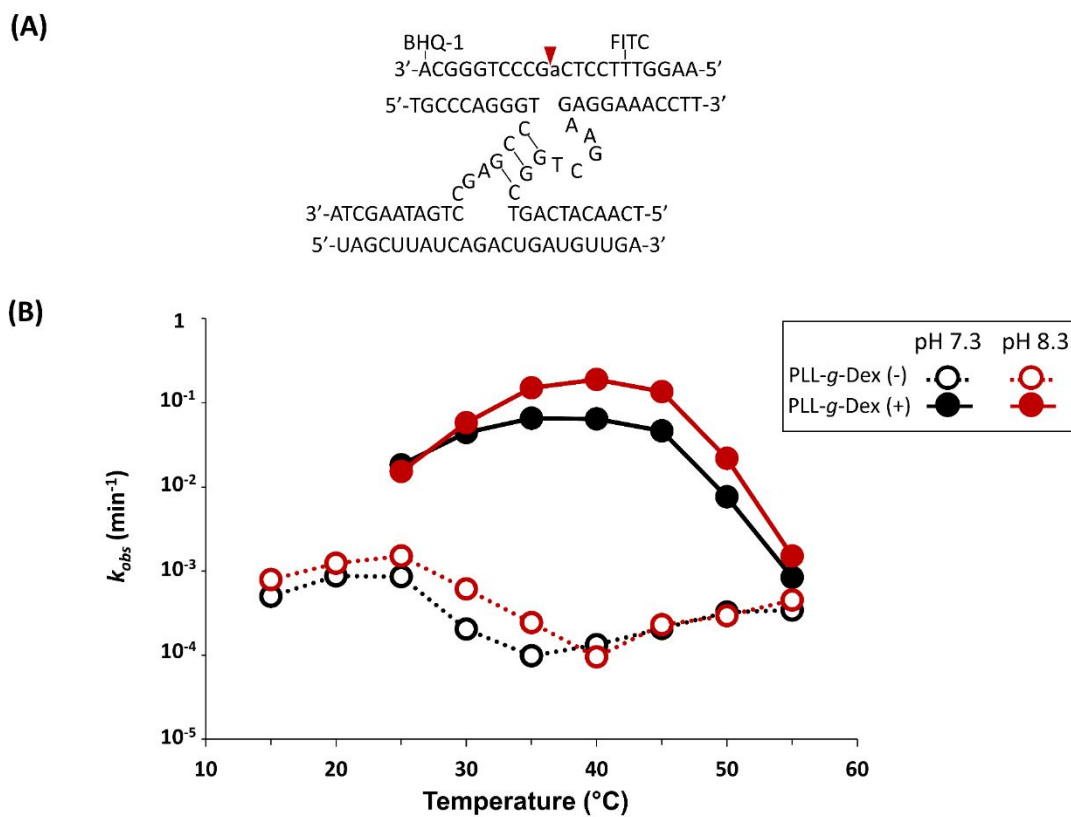
Figure 4. (A) Sequence and locations of fluorophore and quencher on 8-17 MNAzyme substrate and the sequence and structure of the MNAzyme bound to the target miR-21. Lowercase letter denotes a ribonucleotide, and the red triangle indicates the cleavage site on the substrate. (B) Temperature dependence of 8-17 MNAzyme reactions under the multiple-turnover conditions with 0.2 mM Pb^{2+} as a metal ion cofactor in the absence (dotted line) and presence (solid line) of PLL-g-Dex at pH 7.3 (black) and pH 8.3 (red).

The reaction rate of 8-17 MNAzyme can be increased by tuning pH

A study of the Pb^{2+}-dependent 8-17 DNAzyme activity over a range of pH revealed that an increase in pH resulted in a faster reaction rate.[31] The plot of $\log(k_{obs})$ versus pH had a slope of 1.0, which suggests that a single deprotonation at the cleavage site is the rate-limiting step. The mechanism of the DNAzyme-catalyzed cleavage reaction is believed to be metal-assisted general acid-base catalysis.[27] Analysis of the crystal structure of the 8-17 DNAzyme indicates that Pb^{2+} coordinates a water molecule that serves as a general acid to facilitate proton transfer involved in the cleavage reaction.[40]

To the best of our knowledge, there has been no report of the pH dependency of the reaction catalyzed by the 8-17 MNAzyme. We evaluate the 8-17 MNAzyme activity at pH 7.3 and 8.3 (the pK_a of hydrated Pb^{2+} is 7.8[27]). In the presence of PLL-g-Dex, the rate constant at 40 °C was almost 3-fold higher at pH 8.3 (18.8×10^{-2} min^{-1}) than at pH 7.3 (6.42×10^{-2} min^{-1}) (Fig. 4B). This result

shows that the reaction rate of an MNAzyme can be increased by increasing the

pH of the solution above the pK_a of the hydrated metal ion cofactor.

When the pH of the solution is increased, the rate of spontaneous

hydrolysis of the substrate is also increased. Further, the rate constants of the

MNAzyme reaction without miR-21 target were higher in the presence of PLL-g-

Dex than in the absence of the copolymer. Since PLL-g-Dex facilitated

hybridization of the complementary strands, the target-independent

MNAzyme·substrate complex assembly could occur more effectively than in the

absence of the copolymer. However, in the presence of PLL-g-Dex at both pH

7.3 and 8.3, the background signals from the spontaneous hydrolysis of substrate

and target-independent reactions were considerably lower than in the presence

of miR-21 target (Table 1). The highest signal-to-background ratio was observed

at pH 8.3 in the presence of PLL-g-Dex.

Table 1. Rate constants (k_{obs}) of spontaneous hydrolysis reaction (Substrate),

MNAzyme target-independent reaction (Substrate + MNAzyme), and MNAzyme

reaction in the presence of miR-21 target (Substrate + MNAzyme + Target) in the

presence of 0.2 mM Pb^{2+} and signal to background (S/B)

PLL-g-Dex N/P ratio	Temp.	pH	k_{obs} /10⁻² (min⁻¹)			S/B ratio
			Substrate	Substrate + MNAzyme (Background)	Substrate + MNAzyme + Target (Signal)	
0 (No polymer)	25 °C	7.3	0.00	0.02	0.09	4.5
		8.3	0.03	0.03	0.15	5.0
2	40 °C	7.3	0.01	0.09	6.42	71
		8.3	0.04	0.19	18.8	98

Conclusion

We demonstrated that the cationic comb-type copolymer PLL-*g*-Dex increased the reaction rate of 8-17 DNAzymes and 8-17 MNAzymes in experiments designed to detect target nucleic acids under the multiple-turnover conditions. There are three main differences between the 8-17 MNAzyme used in this study and the 10-23 MNAzyme evaluated in our earlier studies.[23,25] The first is the identity of the reactive metal ion cofactor. The 8-17 MNAzyme is more reactive with Pb^{2+} as a cofactor than with Mn^{2+}, whereas the 10-23 MNAzyme is more reactive with Mn^{2+}. The second difference is in the cleavage site sequence requirement. The third difference is in the structure of the catalytic core. The catalytic core of the 8-17 MNAzyme includes stem and loop structures that are more intricate than the structure of the 10-23 MNAzyme. Despite these differences, the cationic copolymer PLL-*g*-Dex enhanced catalytic activity of both in a similar manner: The copolymer facilitated hybridization of the complementary strands and stabilized the nucleic acid complex. We infer that the binding of PLL-*g*-Dex did not distort the inherent catalytic core structure, unlike PAA-*g*-Dex (another cationic comb-type copolymer) and PLL (a cationic homopolymer), which inhibit the substrate cleavage presumably because these polymers disrupt

the catalytically active structures. Importantly, inherent metal ion- and pH-dependences were observed in the presence of PLL-g-Dex. These results imply that the association of the DNA-based enzymes with the copolymer did not significantly influence interaction with the metal ion cofactor. We expect that cationic copolymer-assisted nucleic acid enzymes will find application in development of DNA-based sensors in various fields including the health-care industry.

Conflicts of interest

There are no conflicts of interest to declare.

Acknowledgements

References

1   C. C. Chang, C. C. Chen, S. C. Wei, H. H. Lu, Y. H. Liang and C. W. Lin, *Sensors (Switzerland)*, 2012, **12**, 8319–8337.

2   P. M. Lizardi, X. Huang, Z. Zhu, P. Bray-Ward, D. C. Thomas and D. C. Ward, *Nat. Genet.*, 1998, **19**, 225–232.

3   T. Notomi, H. Okayama, H. Masubuchi, T. Yonekawa, K. Watanabe, N. Amino and T. Hase, *Nucleic Acids Res.*, 2000, **28**, E63–E63.

4   R. R. Breaker and G. F. Joyce, *Chem. Biol.*, 1994, **1**, 223–229.

5   S. W. Santoro and G. F. Joyce, *Proc. Natl. Acad. Sci.*, 1997, **94**, 4262–4266.

6   S. W. Santoro and G. F. Joyce, *Biochemistry*, 1998, **37**, 13330–13342.

7   W. Zhou, R. Saran and J. Liu, *Chem. Rev.*, 2017, **117**, 8272–8325.

8   Y. V. Gerasimova and D. M. Kolpashchikov, *Chem. Biol.*, 2010, **17**, 104–106.

9   E. Mokany, S. M. Bone, P. E. Young, T. B. Doan and A. V. Todd, *J. Am. Chem. Soc.*, 2010, **132**, 1051–1059.

10   P. Zhang, Z. He, C. Wang, J. Chen, J. Zhao, X. Zhu, C. Z. Li, Q. Min and

J. J. Zhu, *ACS Nano*, 2015, **9**, 789–798.

11   X. Li, W. Cheng, D. Li, J. Wu, X. Ding, Q. Cheng and S. Ding, *Biosens.*

Bioelectron., 2016, **80**, 98–104.

12   W. Diao, M. Tang, X. Ding, Y. Zhang, J. Yang, W. Cheng, F. Mo, B. Wen,

L. Xu and Y. Yan, *Microchim. Acta*, 2016, **183**, 2563–2569.

13   K. Zagorovsky and W. C. W. Chan, *Angew. Chemie Int. Ed.*, 2013, **52**,

3168–3171.

14   O. Hanpanich and A. Maruyama, *Polym. J.*, 2019, **51**, 935–943.

15   A. Maruyama, H. Watanabe, A. Ferdous, M. Katoh, T. Ishihara and T.

Akaike, *Bioconjug. Chem.*, 1998, **9**, 292–299.

16   A. Maruyama, Y. Ohnishi, H. Watanabe, H. Torigoe, A. Ferdous and T.

Akaike, *Colloids Surfaces B Biointerfaces*, 1999, **16**, 273–280.

17   A. Maruyama, M. Katoh, T. Ishihara and T. Akaike, *Bioconjug. Chem.*,

1997, **8**, 3–6.

18   R. Moriyama, N. Shimada, A. Kano and A. Maruyama, *Biomaterials*, 2011,

32, 7671–7676.

19   W. J. Kim, T. Dr, T. Prof and A. Prof, *Chem. - A Eur. J.*, 2001, **7**, 176–180.

20   W. J. Kim, T. Akaike and A. Maruyama, *J. Am. Chem. Soc.*, 2002, **124**, 12676–12677.

21   W. J. Kim, Y. Sato, T. Akaike and A. Maruyama, *Nat. Mater.*, 2003, **2**, 815–820.

22   S. W. Choi, N. Makita, S. Inoue, C. Lesoil, A. Yamayoshi, A. Kano, T. Akaike and A. Maruyama, *Nano Lett.*, 2007, **7**, 172–178.

23   J. Gao, N. Shimada and A. Maruyama, *Biomater. Sci.*, 2015, **3**, 308–316.

24   O. Hanpanich, H. Miyaguchi, H. Huang, N. Shimada and A. Maruyama, *Nucleosides, Nucleotides and Nucleic Acids*, 2019, **0**, 1–14.

25   J. Gao, N. Shimada and A. Maruyama, *Biomater. Sci.*, 2015, **3**, 716–720.

26   O. Hanpanich, T. Oyanagi, N. Shimada and A. Maruyama, *Biomaterials*, 2019, **225**, 119535.

27   T. Lan and Y. Lu, in *Interplay between Metal Ions and Nucleic Acids*, eds.

A. Sigel, H. Sigel and R. K. O. Sigel, Springer Netherlands, Dordrecht, 2012, pp. 217–248.

28   S. Du, Y. Li, Z. Chai, W. Shi and J. He, *Bioorg. Chem.*, 2020, **94**, 103401.

29   R. P. . Cruz, J. B. Withers and Y. Li, *Chem. Biol.*, 2004, **11**, 57–67.

30   J. Li, W. Zheng, A. H. Kwon and Y. Lu, *Nucleic Acids Res.*, 2000, **28**, 481–488.

31   A. K. Brown, J. Li, C. M. B. Pavot and Y. Lu, *Biochemistry*, 2003, **42**, 7152–7161.

32   Y. Sato, Y. Kobayashi, T. Kamiya, H. Watanabe, T. Akaike, K. Yoshikawa and A. Maruyama, *Biomaterials*, 2005, **26**, 703–711.

33   N. Ota, M. Warashina, K. N. I. Hirano, K. Hatanaka and K. Taira, *Nucleic Acids Res.*, 1998, **26**, 3385–3391.

34   N. Yamaguchi, Y. K. Zouzumi, N. Shimada, S. I. Nakano, N. Sugimoto, A. Maruyama and D. Miyoshi, *Chem. Commun.*, 2016, **52**, 7446–7449.

35   S. I. Nakano, M. Fujimoto, H. Hara and N. Sugimoto, *Nucleic Acids Res.*, 1999, **27**, 2957–2965.

36   H.-K. Kim, J. Liu, J. Li, N. Nagraj, M. Li, C. M.-B. Pavot and Y. Lu, *J. Am. Chem. Soc.*, 2007, **129**, 6896–6902.

37   J. M. Yoshizawa and D. T. W. Wong, *Methods Mol. Biol.*, 2013, **936**, 313–324.

38   S. Volinia, G. A. Calin, C.-G. Liu, S. Ambs, A. Cimmino, F. Petrocca, R. Visone, M. Iorio, C. Roldo, M. Ferracin, R. L. Prueitt, N. Yanaihara, G. Lanza, A. Scarpa, A. Vecchione, M. Negrini, C. C. Harris and C. M. Croce, *Proc. Natl. Acad. Sci.*, 2006, **103**, 2257–2261.

39   J. Wang, J. Chen and S. Sen, *J. Cell. Physiol.*, 2016, **231**, 25–30.

40   H. Liu, X. Yu, Y. Chen, J. Zhang, B. Wu, L. Zheng, P. Haruehanroengra, R. Wang, S. Li, J. Lin, J. Li, J. Sheng, Z. Huang, J. Ma and J. Gan, *Nat. Commun.*, 2017, **8**, 2006.

Unable to Convert Image

The dimensions of this image (in pixels) are too large
to be converted. For this image to convert,
the total number of pixels (height x width) must be
less than 40,000,000 (40 megapixels).

Figure 1

Unable to Convert Image

The dimensions of this image (in pixels) are too large
to be converted. For this image to convert,
the total number of pixels (height x width) must be
less than 40,000,000 (40 megapixels).

Figure 2

Unable to Convert Image

The dimensions of this image (in pixels) are too large
to be converted. For this image to convert,
the total number of pixels (height x width) must be
less than 40,000,000 (40 megapixels).

Figure 3

Unable to Convert Image

The dimensions of this image (in pixels) are too large
to be converted. For this image to convert,
the total number of pixels (height x width) must be
less than 40,000,000 (40 megapixels).

Figure 4
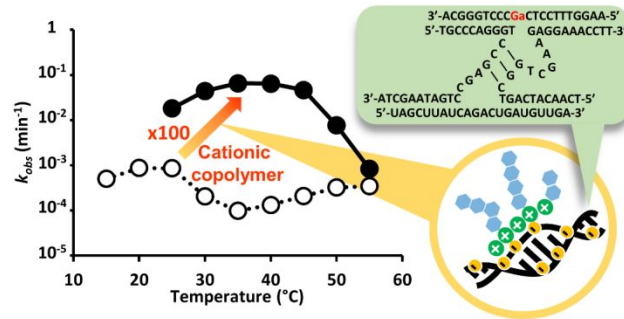
Cationic copolymer acts as chaperone to facilitate multiple strands assembly and enhance nucleic acid enzymes activities.